

Research Article

Conjugation of *E. coli* O157:H7 Antibody to CdSe/ZnS Quantum Dots

N. T. Vo, H. D. Ngo, D. L. Vu, A. P. Duong, and Q. V. Lam

University of Science, Vietnam National University-Ho Chi Minh City, 227 Nguyen Van Cu Street, Ward 4, District 5, Ho Chi Minh City 749000, Vietnam

Correspondence should be addressed to N. T. Vo; vtnthuy@hcmus.edu.vn

Received 15 September 2015; Accepted 16 November 2015

Academic Editor: Daniela Predoi

Copyright © 2015 N. T. Vo et al. This is an open access article distributed under the Creative Commons Attribution License, which permits unrestricted use, distribution, and reproduction in any medium, provided the original work is properly cited.

The conjugation of antibody to semiconductor quantum dots plays a very important role in many applications such as bioimaging, biomarking, and biosensing. In this research, we present some results of highly luminescent core/shell structure CdSe/ZnS on which the *E. coli* antibody was conjugated. The CdSe core was synthesized successfully with chemical “green” method. For biological applications, the capping surfactant, trioctylphosphine oxide, was substituted by a new one, mercaptopropionic acid (MPA), before the antibody attachment step. Finally, the *E. coli* antibody was attached to quantum dots CdSe/ZnS. Morphology, structure, and optical properties were investigated with PL, UV-Vis, TEM, and XRD methods. The successful ligand substitution and antibody attachment were confirmed by zeta potential measurement, FTIR spectroscopy, and TEM. The results showed quantum dots size of 2.3 nm, uniform distribution, and high luminescence. CdSe/ZnS core/shell structure had better stability and enhanced the luminescence efficiency up to threefold compared with the core CdSe. MPA ligand shifted the initial hydrophobic quantum dots to hydrophilic ones, which helped to dissolve them in organic solvents and attach the antibody.

1. Introduction

Colloidal semiconductor quantum dots (QDs) are nanocrystals that have tunable emission through changes in their size. They have attracted huge attention due to the quantum confinement and surface effects. Since last decade, there have been numerous studies on manufacturing and applications of semiconductor nanocrystals, particularly on II-VI compounds, such as CdSe, CdTe, and CdS [1–3]. Among these highly luminescent nanomaterials, CdSe quantum dot is the most popular one thanks to the ease in synthesis. Besides, CdSe is the direct bandgap material with energy value of 1.74 eV, suitability for light emission in the visible spectral range, strong fluorescence, and narrow full width at half maximum (FWHM). Furthermore, compared with organic dyes, the CdSe is of higher reliability and low photobleaching so it can be used to replace organic dyes such as rhodamine 640. With novel optical properties, CdSe quantum dot is an appropriate candidate for applications especially in biology such as biomarkers and biosensors [4]. The QDs-based fluorescent sensing relies on the interaction between antigen

and antibody that are conjugated to semiconductor QDs. The use of fluorescence indicators can help us determine quickly and accurately the bacteria and some viral diseases in liquid media.

Although the CdSe quantum dots have many benefits, they also have several problems such as stability, luminescence intensity and toxicity. When CdSe quantum dots are synthesized with surfactant TOPO, about 70% of nanocrystal surface is Cadmium atom associated with TOPO and the rest 30% of Selenium is in dangling bond status [5]. This not only makes QDs be easily oxidized due to formation of a thin layer of SeO on the crystal surface but also serves as a channel leading to the nonradiative recombination and luminescence efficiency decrement. In addition, if their toxicity is not considered seriously, significant risks can be presented to environment and health under certain conditions particularly for biological applications. The metabolism leads to release of toxic ions (Cd^{2+} and Se^{2-}) and poisons biological environment. To prevent the toxic ions and oxidation of QDs, quantum dots should be coated with nontoxic layers to form core/shell structure.

Coating CdSe quantum dots with another semiconductor material of higher energy bandgap such as CdS, ZnS, and ZnSe lead to electron-hole pair separation in the core material and better surface passivation, thereby helping achieve greater chemical stability and enhance photoluminescence intensity [6, 7]. Comparatively, a thin layer of ZnS surrounding CdSe quantum dots can help improve quantum yield of CdSe/ZnS core shell up to 70% compared with bare CdSe case [4]. For ZnS coating, successive ion layer adsorption and reaction (SILAR) method has been employed. The precursor solution of Zn^{2+} and S^{2-} in TOP, TOPO solvents are injected into the CdSe quantum dots solution consecutively.

In synthesis process of CdSe/ZnS core/shell, trioctylphosphine oxide (TOPO) and trioctylphosphine (TOP) play role as capping surfactants. They help retain the hydrophobic character of quantum dots and hence the QDs are insoluble in water, which prevents quantum dots from biological applications. Therefore, ligand exchange in order to apply quantum dots in biodetection is an absolute necessity. There are different methods to modify the surface of quantum dots and ligand exchange method is the most common one. The hydrophobic organic ligand can be replaced by hydrophilic thiols or polymer. This process helps to disperse quantum dots well in water and strengthen biocompatibility [8]. In this work, the CdSe cores were synthesized with chemical “green” method. They were coated with ZnS shell via the successive ion layer adsorption and reaction method (SILAR) method. For the employment of QDs in biotechnology, we substituted the capping agents, TOPO, with mercaptopropionic acid (MPA). After that, the *Escherichia coli* (*E. coli*) antibody was attached to quantum dots CdSe/ZnS-MPA. In order to characterize the structural phase and optical properties of the obtained samples, we used X-ray diffraction (XRD), absorption photoluminescence (PL) spectroscopy methods, and TEM. The successful ligand substitution and antibody attachment were confirmed by FTIR spectroscopy, TEM, PL, and zeta potential techniques. In this study, we aimed at the optimal process for the synthesis of high quality quantum dots so that they could be applied in biology. These results highlighted the advantage of spectroscopy methods to verify the conjugation between QDs and antibody.

2. Experimental

2.1. Synthesis of CdSe Core. Chemical substances for the synthesis of CdSe QDs are cadmium acetate dehydrate, selenium powder (Se, 99.5%), diphenyl ether (DPE), methanol, toluene of Merck, trioctylphosphine (TOP), 1-octadecene (ODE, 90%) of Acros, trioctylphosphine oxide (TOPO) of Aldrich, oleic acid (OA, 90%) of Fisher, and hexane of Scharlau. All chemicals were used without additional purification.

The synthesis of CdSe QDs followed the route 0.133 g of cadmium acetate dehydrates and 0.64 mL of OA was dissolved in 5 mL of DPE. The reaction mixture was heated at 120°C with constant stirring for 30 minutes in a continuous nitrogen stream to remove water and acetic acid. Then we maintained the temperature at 120–180°C, called reaction temperature, and 0.5 mL trioctylphosphine selenide (TOP-Se) 1M was quickly injected into the reaction mixture.

After injection, the solution began changing its colour, from transparent to red. At desired time intervals, the reaction solution was cooled down to room temperature.

2.2. Synthesis of CdSe/ZnS Core/Shell Structure. To passivate surface dangling bonds and stabilize photophysical characteristics of CdSe QDs, we covered the CdSe core with shells by ion layer adsorption and reaction (SILAR) technique [2, 6]. A 0.04 M zinc precursor was a mixture of 43.9 mg zinc acetate dehydrate, 0.25 g TOPO, 1 mL TOP, and 4 mL ODE and then was heated up to 200°C. On the other hand, a sulphide solution 0.04 M was formed by dissolving 6.4 mg sulphur and 5 mL TOP.

We prepared a solution of 2 mL of CdSe quantum dot ($\sim 5.6 \cdot 10^{-5}$ mol), hexane, and 3 mL ODE. Then we fabricated shells by increasing the temperature gradually.

At 120°C, we injected 1.237 mL zinc precursor into CdSe QDs solution and kept it for 10 minutes.

At 140°C, we injected 0.247 mL sulphide solution and kept it for 10 minutes.

At 160°C, we injected 1.742 mL zinc precursor and kept it for 10 minutes and finally added 0.348 mL sulphide solution and kept it for 10 minutes.

2.3. Structural and Optical Characterizations. Powder X-ray diffraction using Cu $K\alpha$ radiation (Model XRD D8-ADVANCE) was performed for analysis of structure of CdSe/ZnS QDs. The morphology and crystallinity of the core/shell QDs were investigated by transmission electron microscopy. Room temperature UV-Vis absorption spectra (Model UV-VIS Jacob V-670) with the wavelength range of 400–900 nm and the photoluminescence spectroscopy (Horiba Jobin Yvon, USA Fluorescence Spectrometer) with the excitation wavelength 325 nm were employed to analyse optical properties of quantum dots.

2.4. Ligand Exchange of Quantum Dots with MPA. After the synthesis of TOPO-capped CdSe/ZnS QDs, TOPO was replaced with mercaptopropionic acid (MPA) to make them soluble in phosphate buffer solution (PBS). With the carboxylate ligand existing in the molecules, MPA provided the water solubility to QDs. Typical 5 μL of MPA and 1 mL of pH buffer were poured into 1 mL of CdSe/ZnS quantum dots-containing solution and stirred for 24–48 hours. The quantum dots were rinsed and centrifuged three times to remove MPA residue.

2.5. Bioconjugation of Quantum Dots with Antibody *E. coli* O157:H7. 40 μL sulfo-NHS and 40 μL 1-ethyl-3-(3-dimethylaminopropyl) carbodiimide (EDC) were added into 1 mL CdSe/ZnS-MPA solution. The solution was shaken for 2 hours at room temperature to induce coupling reaction. Sulfo-NHS-terminated CdSe/ZnS quantum dots were collected by centrifugation and dispersed in the buffer solution, and then antibody *E. coli* O157:H7 was added. The mixture was incubated for 24 hours with shaking. When the conjugation of CdSe/ZnS quantum dots with antibody was

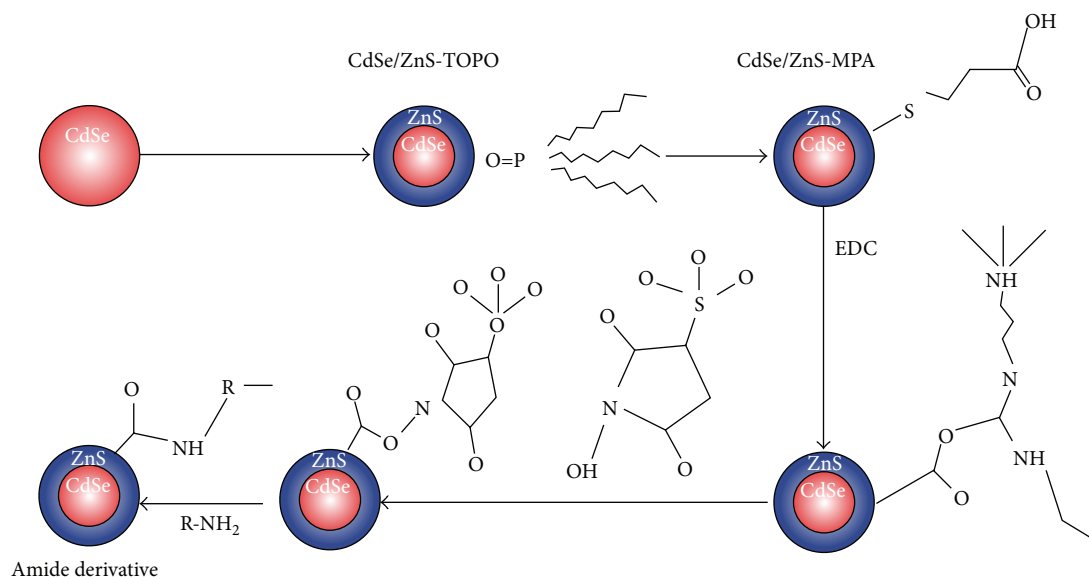


FIGURE 1: The bioconjugation procedure of CdSe/ZnS quantum dots.

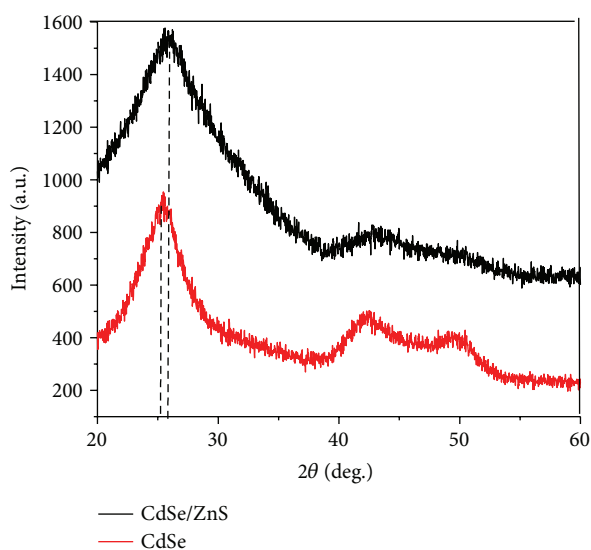


FIGURE 2: XRD patterns of CdSe and CdSe/ZnS quantum dots.

completed, the QDs in solution were obtained by centrifugation and these particles were cleaned and dispersed in PBS solution. They were stored in a refrigerator to be preserved for later use.

Figure 1 shows the whole process of surface modification and bioconjugation of quantum dots with antibody.

3. Results and Discussion

3.1. Structure and Crystallinity of Quantum Dots. Figure 2 showed XRD patterns of CdSe and CdSe/ZnS semiconductor quantum dots synthesized for 10 minutes at 150°C. Three main diffraction peaks could be spotted in the graph, which

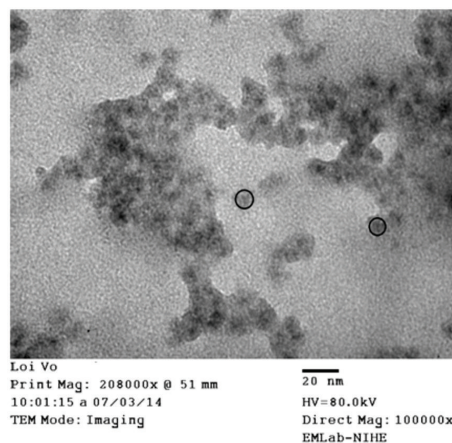


FIGURE 3: TEM image of CdSe/ZnS core/shell sample coated at 150°C.

can be indexed as (111), (220), and (311) diffraction peaks of the cubic zinc blende CdSe corresponding to three diffraction angles (2θ) 26.1°, 43.8°, and 51.7°.

The clear diffraction peaks indicated that the CdSe QDs crystallized well in zinc blende structure. XRD peaks of CdSe/ZnS core/shells shifted to higher 2θ angles compared with the reference PDF card (#65-0309). This shift was induced from the compressive strain of CdSe core by ZnS shell. Since ZnS had the smaller lattice parameter ($a = 3.777 \text{ \AA}$, $c = 6.188 \text{ \AA}$) than CdSe ($a = 4.299 \text{ \AA}$, $c = 7.010 \text{ \AA}$), the core CdSe had been compressed under ZnS shell coating process.

Figure 3 showed TEM image of CdSe/ZnS quantum dots. Nanoparticles were spherical in shape and well dispersive. The average size of CdSe/ZnS was estimated about 4 nm and they showed narrow size distribution. Besides, we also could

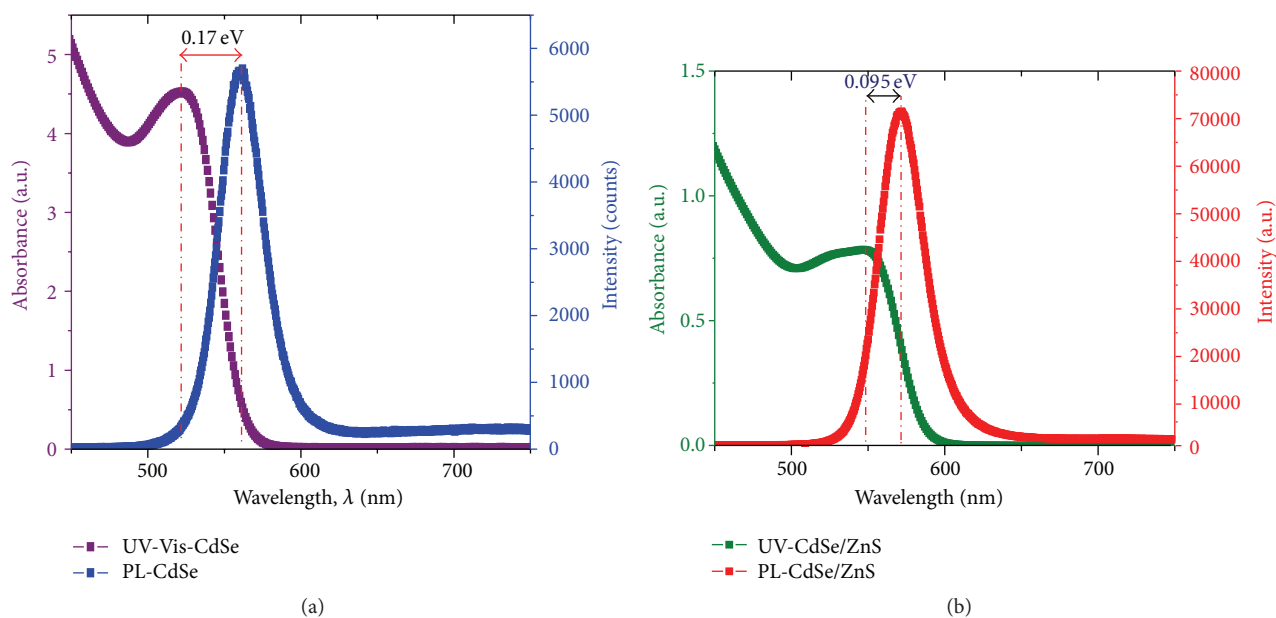


FIGURE 4: UV-visible absorption and PL of CdSe (a) and CdSe/ZnS (b).

see the light grey shell of ZnS surrounding the dark CdSe core. Figures 2 and 3 confirmed indirectly the successful formation of the core-shell structure CdSe/ZnS.

3.2. Optical Properties of CdSe/ZnS Quantum Dots. Figure 4 showed UV-visible light absorption and PL spectra from CdSe and CdSe/ZnS core/shell structure quantum dots.

Both absorption and emission spectra of CdSe and CdSe/ZnS showed the blue shift of the peaks considering the energy bandgap of CdSe (1.74 eV~713 nm). This blue shift originated from quantum dots confinement effect as the sizes of nanoparticles decreased below Bohr's radius.

In Figure 4(b), the luminescence intensity of CdSe/ZnS sample increased and the Stoke shift of quantum dots was smaller than CdSe sample. Furthermore, cloud surface emission in the long wavelength (from 620 nm) went down drastically close to 0. This demonstrated that the CdSe surface traps had been passivated successfully by ZnS shells.

3.3. Ligand Exchange of CdSe/ZnS. CdSe/ZnS quantum dots were synthesized using a nonpolar surfactant TOPO. Thus, surface modification was needed to resolve water insolubility and bioincompatibility problems of quantum dots. This could be done by replacing TOPO with MPA, whose molecular structure is comprised of thiol (-SH) and carboxyl groups. The ligand exchange for quantum dots is possible because of the two functional groups, thiol and carboxyl groups. The thiol group had strong electron affinity to the zinc in the ZnS shell, and thus surface TOPO could be replaced with MPA. Carboxyl groups had excellent hydrophilic property needed for water solubility and they also provided reactive sites for immobilization biological agents. Figure 5 showed FTIR spectra of CdSe/ZnS, MPA, and CdSe/ZnS-MPA samples over range from 500 to 4000 cm^{-1} .

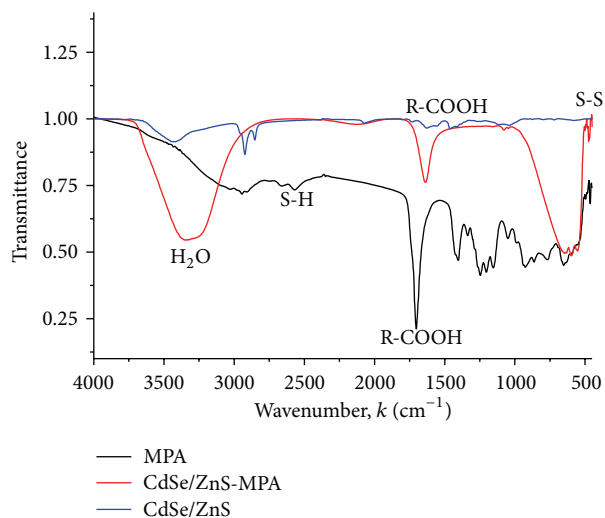


FIGURE 5: FTIR spectra of MPA-capped CdSe/ZnS QDs.

Figure 5 showed a prominent absorption band at $1702 \pm 10 \text{ cm}^{-1}$ in MPA and CdSe/ZnS-MPA which was due to the C=O stretch of carboxyl group. The absorption band due to carboxyl group for CdSe/ZnS-MPA shifted to lower energy. The appearance of the vibration band due to carboxyl group and disulfide stretch (at 500 cm^{-1}) in CdSe/ZnS-MPA sample indicated that the carboxyl group was not involved in coordination to the quantum dots surface and MPA was attached to Cd ion on the surface of QDs through the thiol groups. In addition, the appearance of 2557 cm^{-1} peak in the IR spectra of MPA was oscillation mode of -SH, but it was not observed in the spectra of CdSe/ZnS and CdSe/ZnS-MPA samples; this proved that the thiol groups (-SH)

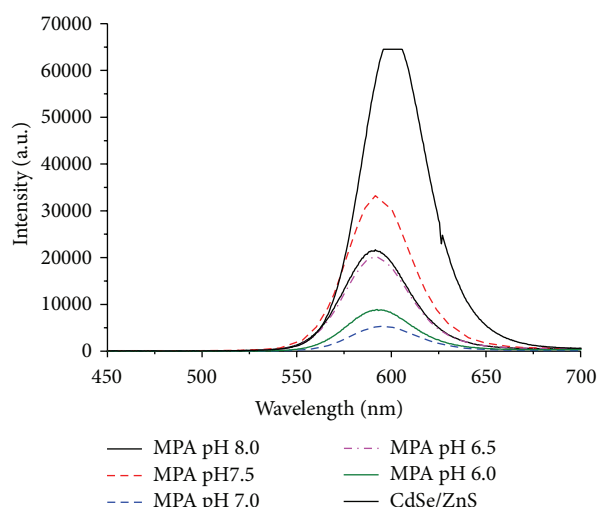


FIGURE 6: The change in PL intensity of CdSe/ZnS-MPA as a function of pH.

reacted with the surface of quantum dots. Vibrations at 2957 and 3300 cm^{-1} due to hydroxyl ($-\text{OH}$) group existed in MPA and CdSe/ZnS-MPA samples and disappeared in CdSe/ZnS sample. This confirmed that we succeeded in ligand exchange and Qds were water soluble and biocompatible.

PL spectra of CdSe/ZnS NCs capped by MPA were shown in Figure 6.

The PL spectra of CdSe/ZnS-MPA showed the blue shift of the peaks compared with CdSe/ZnS case. This blue shift originated from the size difference between MPA and TOPO molecules. Since the size of MPA was smaller than that of TOPO, the size of Qds became much smaller when TOPO was replaced by MPA. Moreover, the change in PL intensity of Qds as a function of pH indicates that the value of 7.5 was best for conjugating quantum dots to biological agents. In base environment, the binding between Cd and Zn became much better and absorbance as well as luminescence intensity increased excessively. Cd^{2+} and Zn^{2+} ions precipitated in base environment of pH 8.5–9.0, the Cd and Zn ions were passivated, and PL intensity reduced.

3.4. Bioconjugation of CdSe/ZnS Capped MPA with *E. coli* O157:H7 Antibody. To conjugate CdSe/ZnS-MPA with antibody, we used covalent cross-linking method. First, 1-ethyl-3-(3-dimethylaminopropyl) carbodiimide (EDC) was mixed with *n*-hydroxysulfosuccinimide (sulfo-NHS). Next, the carboxyl groups in MPA at the surface of CdSe/ZnS-MPA Qds were esterified by sulfo-NHS through EDC/NHS coupling reaction and formed NHS-activated acid. When antibodies were injected to the above protocol, NHS groups at the surface of Qds were replaced with amino groups in the antibody molecules to form amide bond. The zeta potential and FTIR spectra were used to investigate this conjugation.

As can be seen in Figure 7, the zeta potential of CdSe/ZnS capped MPA was shifted after conjugating antibody. This could be explained that the surfaces of MPA-capped quantum dots were surrounded by negative charges. The value of

the zeta potential was approximately -30.2 mV at peak. When conjugating antibody to quantum dots the molecular lengths and the surface charges of Qds were changed. This proved that the bioconjugation proceeded successfully. *E. coli* O157:H7 antibody had been attached well to CdSe/ZnS-MPA structure.

As illustrated in Figure 1 antibody agents were conjugated to Qds through amide bonding. However, in Figure 8, FTIR spectra of Qds-MPA and Qds-MPA-antibody seemed to be very similar in shapes since the vibration frequency of amide group was adjacent to the one of carboxyl group. So, the first derivatives of those two spectra were taken in range of 1000 to 2000 cm^{-1} with regard to certifying the amide bonding.

According to the derivative results in Figure 9, at 1500 – 1560 cm^{-1} , the bonding of amide group onto MPA could be validated at a certain level of certainty. Small peaks could be found in that wave number range (dashed rectangle) in Qds-MPA-antibody case but not in Qds-MPA counterpart. Such peaks could not be seen in sharp and high pattern because the number of bonding was not that much.

TEM microscopy was employed to evaluate the morphology variation of Qds conjugated with antibody. In Figure 10, it could be easily seen that sizes and shapes of final products had changed drastically from less than 20 nm of CdSe/ZnS core/shell to nearly 1 micrometer of CdSe/ZnS-MPA-antibody.

Figure 11 illustrated photoluminescence spectra of CdSe/ZnS-MPA conjugated antibody (solid line) and nonconjugated antibody (short dashed line) with maximum emission peaks at 596 nm and 604 nm , respectively. The FWHM of peaks were relatively narrow; it proved low size distribution in both cases. Besides, the PL peak of Qds-antibody had shifted to blue side of about 7 nm . This was due to the alteration of surface coating around the Qds-MPA after being conjugated with antibodies. It led to the reduction of the surface charges and the directional polarizability of molecules surrounding the Qds and led to the blue shift of emission peak. In additionally, the fluorescence quenching was observed in Qds-MPA-antibody sample. This could be due to the formation of antibody on the surface of quantum dots.

4. Conclusions

We succeeded in synthesizing CdSe quantum dots with chemical green method. The CdSe quantum dots were coated with ZnS layers with SILAR method to form core/shell structure which was confirmed through TEM, XRD, PL, and absorption spectra. The capping agent, TOPO, was replaced by MPA in order to obtain water solubility and biological compatibility. After ligand exchange, *E. coli* antibody O157:H7 was conjugated to surface of quantum dots activated by EDC and NHS coupling reaction. This can be considered the most fundamental step in biosensor fabrication, which leads to further application of biosensors. Other kinds of antibodies could be attached to activated quantum dots to broaden the sensing capability. Success of such substitution and bioconjugation was proved by FTIR, zeta potential, TEM,

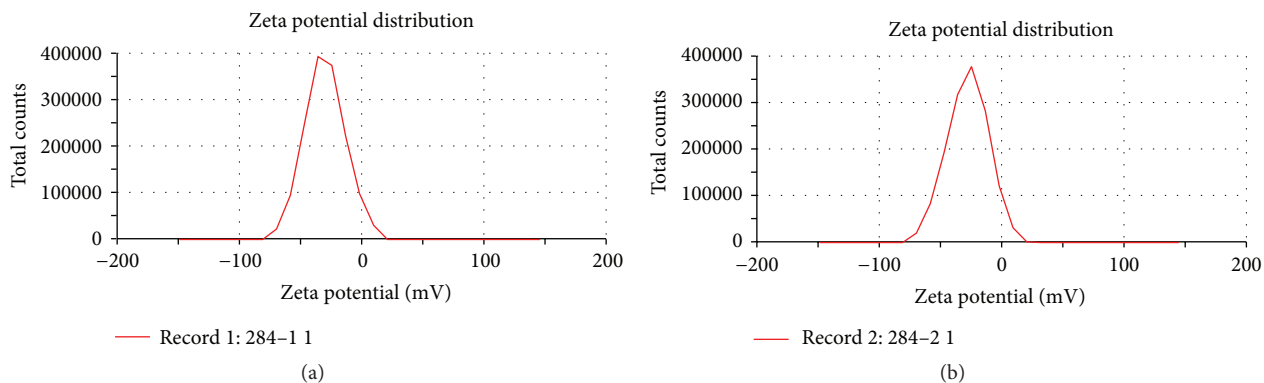


FIGURE 7: The zeta potential of CdSe/ZnS-MPA (a) and CdSe/ZnS-MPA-antibody (b).

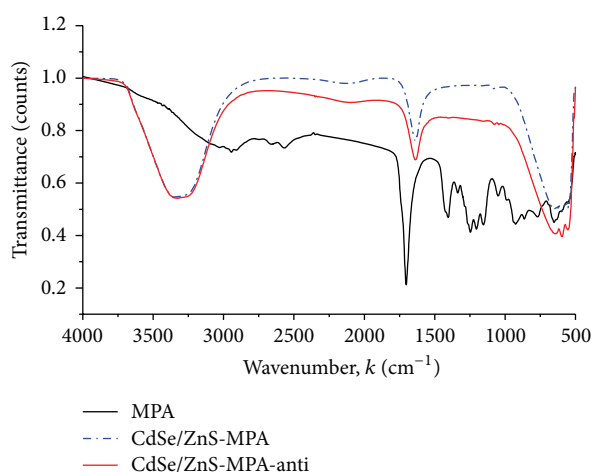


FIGURE 8: FTIR spectra of quantum dots conjugated antibody.

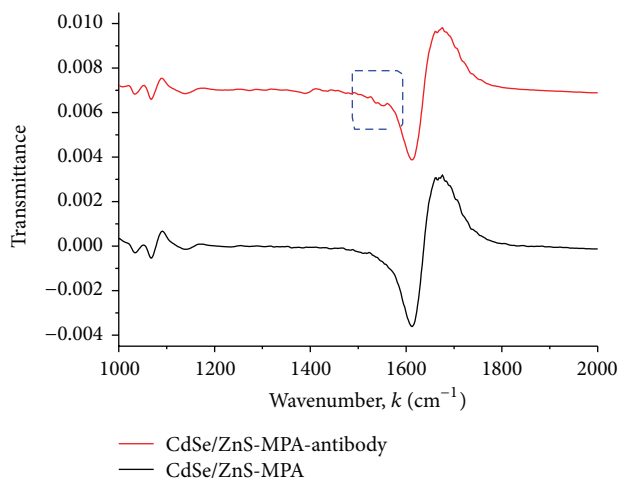


FIGURE 9: First derivative of FTIR spectra of CdSe/ZnS-MPA and CdSe/ZnS-MPA-antibody.

and PL spectra. These results proved the important role of the optical method in verification of the Qds-antibody

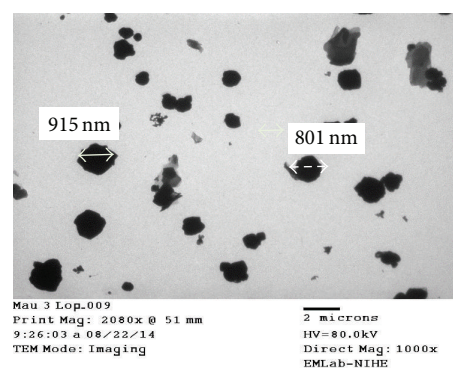


FIGURE 10: TEM image of quantum dots conjugated antibody.

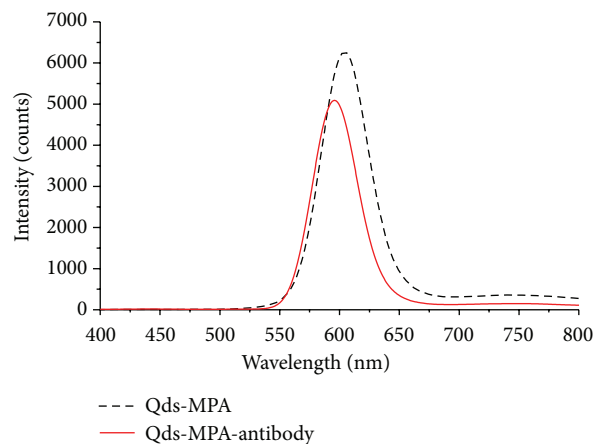


FIGURE 11: Photoluminescence spectra of Qds conjugated antibody.

conjugation and open new approach for the detection of different bacterium. This will be done in further works.

Conflict of Interests

The authors declare that they have no conflict of interests.

Acknowledgment

This work was supported by the Priming Scientific Research Foundation, Grant C from Viet Nam National University in Ho Chi Minh City, Project no. C2016-18-3.

References

- [1] J. Park, J. Joo, S. G. Kwon, Y. Jang, and T. Hyeon, "Synthesis of monodisperse spherical nanocrystals," *Angewandte Chemie International Edition*, vol. 46, no. 25, pp. 4630–4660, 2007.
- [2] X. Wang, X. Loua, Y. Wang et al., "QDs-DNA nanosensor for the detection of hepatitis B virus DNA and the single-base mutants," *Biosensors and Bioelectronics*, vol. 25, no. 8, pp. 1934–1940, 2010.
- [3] R. B. Vasiliev, S. G. Dorofeev, D. N. Dirin, D. A. Belov, and T. A. Kuznetsova, "Synthesis and optical properties of PbSe and CdSe colloidal quantum dots capped with oleic acid," *Mendeleev Communications*, vol. 14, no. 4, pp. 169–171, 2004.
- [4] P. Reiss, M. Protière, and L. Li, "Core/shell semiconductor nanocrystals," *Small*, vol. 5, no. 2, pp. 154–168, 2009.
- [5] J. Taylor, T. Kippeny, and S. J. Rosenthal, "Surface stoichiometry of CdSe nanocrystals determined by rutherford backscattering spectroscopy," *Journal of Cluster Science*, vol. 12, no. 4, pp. 571–582, 2001.
- [6] A. V. Baranov, Y. P. Rakovich, J. F. Donegan et al., "Effect of ZnS shell thickness on the phonon spectra in CdSe quantum dots," *Physical Review B*, vol. 68, no. 16, Article ID 165306, 2003.
- [7] H. Zhu, A. Prakash, D. N. Benoit, C. J. Jones, and V. L. Colvin, "Low temperature synthesis of ZnS and CdZnS shells on CdSe quantum dots," *Nanotechnology*, vol. 21, no. 25, Article ID 255604, 2010.
- [8] R. A. Sperling, W. J. Parak, and R. Soc, "Surface modification, functionalization and bioconjugation of colloidal inorganic nanoparticles," *Philosophical Transactions of the Royal Society A: Mathematical, Physical and Engineering Sciences*, vol. 368, no. 1915, pp. 1333–1383, 2010.

